Heme–Copper/Dioxygen Adduct Formation, Properties, and Reactivity

EDUARDO E. CHUFÁN, SIMONA C. PUIU, AND KENNETH D. KARLIN*

Department of Chemistry, Johns Hopkins University, Baltimore, Maryland 21218

Received February 12, 2007

ABSTRACT

This Account focuses on our recent developments in synthetic heme/copper/O_2 chemistry, potentially relevant to the mechanism of action of heme–copper oxidases (e.g., cytochrome *c* oxidase) and to dioxygen activation chemistry. Methods for the generation of O_2 adducts, which are high-spin heme(Fe^{III})–peroxo–Cu^{II} complexes, are described, along with a detailed structural/electronic characterization of one example. The coordination mode of the O_2-derived heme–Cu bridging group depends upon the copper–ligand environment, resulting in μ-(O_2^{2-}) side-on to Fe^{III} and end-on to Cu^{II} (μ-η^2:η^1) binding for cases having N_4 tetradentate ligands but side-on/side-on (μ-η^2:η^2) μ-peroxo coordination with tridentate copper chelates. The dynamics of the generation of Fe^{III}–(O_2^{2-})–Cu^{II} complexes are known in some cases, including the initial formation of a short-lived superoxo (heme)Fe^{III}($O_2^{\bullet-}$) intermediate. Complexes with cross-linked imidazole–phenol "cofactors" adjacent to the copper centers have also been described. Essential investigations of heme–copper-mediated reductive O–O bond cleavage chemistry are ongoing.

Introduction

The allure of the highly pigmented heme prosthetic groups found in our own blood oxygen-carrier hemoglobin and cytochrome P450 monooxygenases (P450) has historically stimulated interest in heme/O_2 chemistry.[1] While there has been a long time interest in copper ion (and complexes) as reagents for oxidative transformations of synthetic utility, the probing of copper(I) complex dioxygen reactivity with a relevance toward copper proteins (e.g., O_2-carrier hemocyanins, copper monooxygenases, or oxidases) is more recent.[2–5]

This Account, in a sense, focuses on a melding of these two subjects, heme/O_2 and copper/O_2 coordination chemistries. From (a part of) our own research programs, this has led to the generation of a series of heme–copper/O_2 adducts, in fact, Fe^{III}–peroxide(O_2^{2-})–Cu^{II} complexes (**1**–**5** in Chart 1). Such heterobinuclear assemblies are inherently interesting entities, because they comprise new classes of species made up of two redox-active metal ions bridged by an O_2-derived ligand.

The inspiration for our studies comes from the existence of ubiquitous aerobic organism heme–copper oxidases, including cytochrome *c* oxidase (C*c*O).[6,7] These possess a key binuclear active site, with heme (a_3) and a proximal (~4.4–5.3 Å) copper ion (Cu_B) (see Chart 1), where the reduction of dioxygen is coupled to enzyme proton translocation across the membrane (eq 1) in which the enzyme resides, with the resulting proton/charge gradient utilized by ATP synthetase. In short, metabolism of foodstuffs (respiration) leads to the production of reducing equivalents (reduced cytochrome *c*), which react with dioxygen breathed in and is transported to the C*c*O active site; the overall result is the transduction of the thermodynamically available energy (from O_2 reduction to water), leading to the biosynthesis of ATP as the critical form of transportable and utilizable energy for the organism.

$$O_2 + 4e^-(\text{cyt } c) + 8H^+_{in} \rightarrow 2H_2O + 4H^+_{out} \qquad (1)$$

As for any metalloprotein, the reactions occurring at this heme–Cu center cannot be divorced from the inherent chemistry of the metal ions. Our interests,[6] as well as that research coming from complementary investigations by Collman et al.[7] and Naruta et al.,[8,9] consist of the design, generation, and interrogation of small-molecule model systems. Their study may serve to sharpen or focus relevant questions (and answers) about the protein active-site structure and mechanism of the reaction. Elucidation of the synergism between Cu/O_2 and heme/O_2 chemistries as pertains to C*c*O O_2 binding and reduction is a significant goal. How/why is the CcO active site perfectly suited for O_2-reductive cleavage? Why are there three $N_{imidazole}$ ligands (Chart 1) for copper; what is the purpose/function of the His–Tyr cross-link; and why are the active-site iron and copper juxtaposed at ~5 Å (Chart 1)? How is C*c*O chemistry the same or different than seen for multicopper oxidases (affecting the four-electron reduction of O_2) or heme-only P450s or peroxidases?[1]

Practical or fundamental considerations pertaining to heme/Cu/O_2 chemical studies relate to fuel-cell applications, i.e., the reductive cleavage of O_2 to water at a cathode with a catalyst; such efforts have been promulgated by Collman

Eduardo E. Chufán was born in San Juan, Argentina, in 1967. He received his Ph.D. degree in 1999 from the National University of San Luis (Argentina) under the direction of José C. Pedregosa, working on metal–drug complexes. In 2000, he joined the research group of Kenneth D. Karlin at Johns Hopkins University (Baltimore, MD) to work on heme/Cu/dioxygen chemistry. He is currently a postdoctoral fellow at the Johns Hopkins School of Medicine with L. Mario Amzel. His research interests include metal-mediated dioxygen activation and metalloprotein X-ray crystallography.

Simona C. Puiu (born in Cluj-Napoca, Romania) received her B.S. and M.Sc. degrees in chemistry from Babes-Bolyai University, Cluj-Napoca, Romania, in 1995 and 1996, respectively. She then held a position of Research Assistant at the "Raluca Ripan" Institute of Chemistry (1996–1998). She received a Ph.D. degree in inorganic chemistry from Georgetown University, under the supervision of Professor Timothy H. Warren (2004) and is currently working as a postdoctoral researcher at Johns Hopkins University with Professor Kenneth D. Karlin. Her current research interests include the reactivity of synthetic heme and copper complexes with molecular oxygen and/or nitric oxide.

Kenneth D. Karlin is Ira Remsen Professor of Chemistry at John Hopkins University. His copper–dioxygen chemistry interests and research program were developed while at the State University of New York at Albany (1977–1989). He received his Ph.D. degree with Stephen J. Lippard from Columbia University (1975), and he was a NATO postdoctoral Fellow at the University of Cambridge with Jack Lewis and Brian Johnson. His research spans biologically inspired coordination chemistry of copper and heme–copper systems with dioxygen and nitrogen oxides. Additional research interests include metal–complex interactions with DNA and peptides.

* To whom correspondence should be addressed. E-mail: karlin@jhu.edu.

10.1021/ar700031t CCC: $37.00
Published on Web 06/06/2007

Chart 1

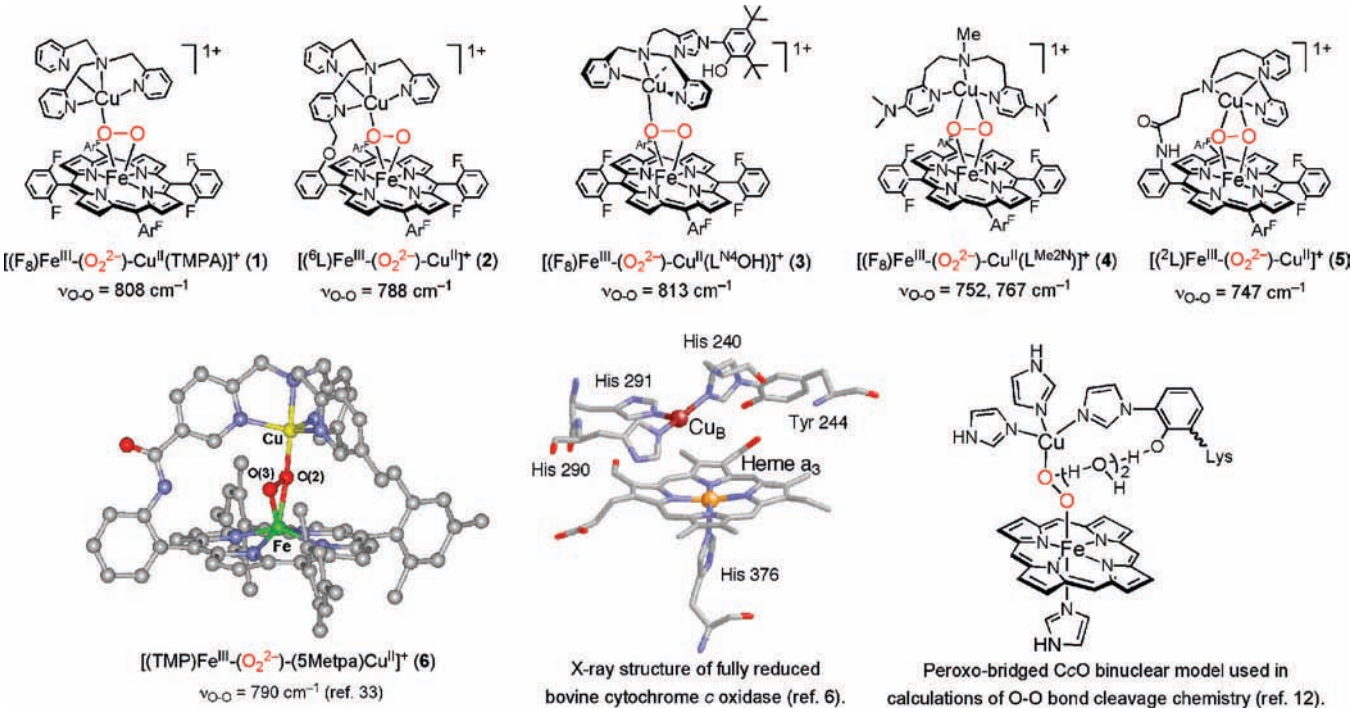

Scheme 1

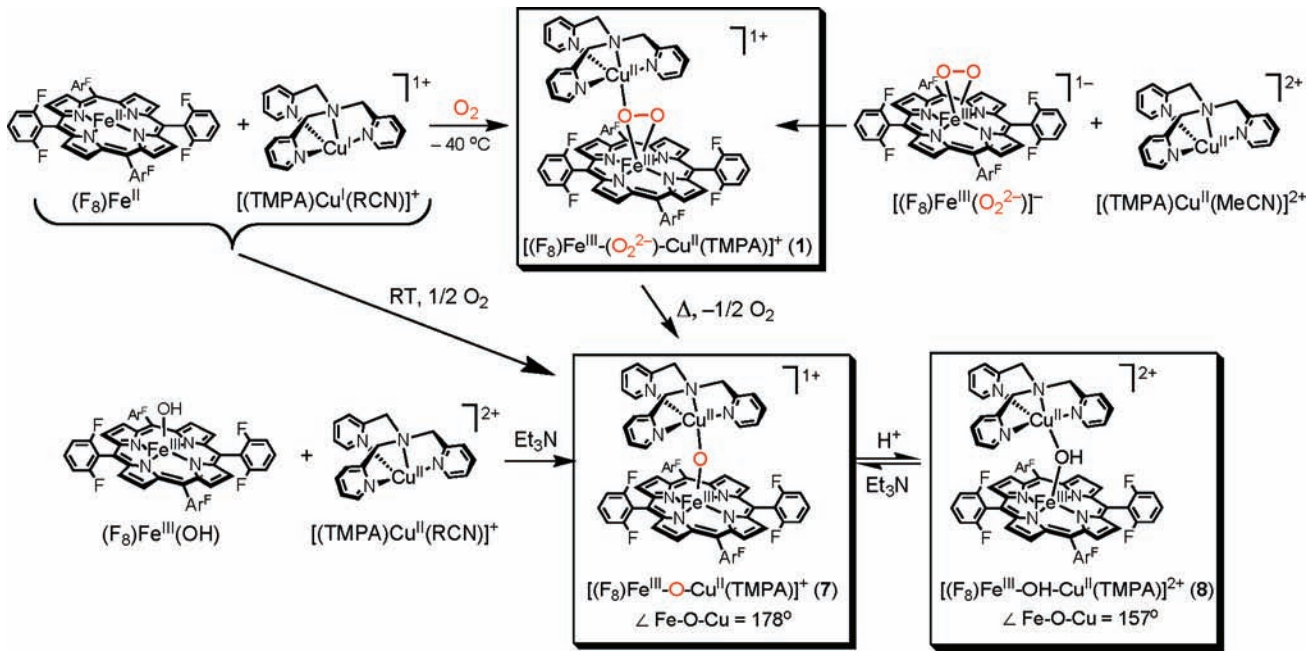

et al.[7] Further, dioxygen activation,[10,11] including metal-ion-mediated enhancement of the substrate oxidation/oxygenation reactivity of ground-state (triplet) O_2, necessarily involves eventual O–O bond reductive cleavage. Thus, any research leading to insights into this process has considerable fundamental importance.[11,12]

Initial Heme–Fe^{II}/Ligand–Cu^{I}/O_2 Reactivity; Fe^{III}–Oxo–Cu^{II} Complexes

Historically, attempts at modeling the C*c*O heme–copper active site typically focused on structural models for the oxidized "resting" state and the generation of Fe^{III}–Cu^{II} complexes with various bridging ligands.[13] Our own initial discovery involving dioxygen chemistry came when we reacted a porphyrinate–iron(II) complex, $(F_8)Fe^{II}$ or $(F_8)Fe^{II}(pip)_2$ (pip = piperidine), with O_2 in the presence of 1 equiv of $[(TMPA)Cu^{I}(MeCN)]^+$ (Scheme 1); the latter was chosen because we had separately established its independent Cu^{I}/O_2 chemistry.[14] The product was the novel μ-oxo complex $[(F_8)Fe^{III}–O–Cu^{II}(TMPA)]^+$ (**7**), with the μ-oxo ligand derived from molecular oxygen; a new isotope-sensitive infrared band appeared at 856 cm^{-1}.[6,15,16]

Table 1. Core Structural Parameters (Å) for Heme–X–Copper Complexes (X = O_2^{2-}, O^{2-}, or OH^-)

heme–X–copper compound	method	Fe···Cu	Fe–O	Cu–O	Fe–X–Cu	reference
$[(F_8)Fe^{III}–(O_2^{2-})–Cu^{II}(TMPA)]^+$ (**1**)	EXAFS	3.72	1.94	1.87	150	26
$[(P)Fe^{III}–(O_2^{2-})–Cu^{II}(TMPA)]^+$	DFT[a]	4.01	1.88 2.07	1.96	170	26
$[(P)Fe^{III}–(O_2^{2-})–Cu^{II}(TMPA)]^+$	DFT[b]	3.70	1.89 1.90	1.85	161	26
$[(F_8)Fe^{III}–O–Cu^{II}(TMPA)]^+$ (**7**)	X-ray	3.60	1.74	1.86	178	15
$[(F_8)Fe^{III}–O–Cu^{II}(TMPA)]^+$ (**7**)	EXAFS	3.55	1.72	1.83	176	19
$[(F_8)Fe^{III}–(OH^-)–Cu^{II}(TMPA)]^{2+}$ (**8**)	EXAFS	3.66	1.87	1.89	157	19
$[(TMP)Fe^{III}–(O_2^{2-})–Cu^{II}(5Metpa)]^+$ (**6**)	X-ray	3.92	2.03 1.89	1.92	166	33
$[(^6L)Fe^{III}–(O_2^{2-})–Cu^{II}]^+$ (**2**)	EXAFS	3.97	1.84	1.84		26, 34
$[(^2L)Fe^{III}–(O_2^{2-})–Cu^{II}]^+$ (**5**)	EXAFS	~3.6	~1.9	1.90		35

[a] Density functional theory (DFT) fully optimized structure. [b] Structure with constrained Fe···Cu = 3.7 Å.

The finding was surprising, given the substantial thermodynamic stability of widely known μ-oxo complexes $(P)Fe^{III}–O–Fe^{III}(P)$ (P = porphryinate). In fact, we and Lee and Holm[17] have shown that such μ-oxo heme–copper complexes are kinetically stable and can also be formed by self-assembly synthesis, such as by adding $(F_8)Fe^{III}$–OH to $[(TMPA)Cu^{II}(MeCN)]^{2+}$ plus triethylamine (Scheme 1).[6]

The X-ray structure of $[(F_8)Fe^{III}–O–Cu^{II}(TMPA)]^+$ (**7**) reveals a linear $Fe^{III}–O–Cu^{II}$ coordination ($\angle$Fe–O–Cu = 178.2°), with very short Fe–O (1.740 Å) and Cu–O (1.856 Å) bonds.[15] Mössbauer spectroscopy and magnetic susceptibility measurements indicate that **7** is a S = 2 system, with high-spin iron(III) strongly antiferromagnetically coupled [$J = -87$ cm^{-1} (solid), where $H = -2JS_1S_2$] to a S = $^1/_2$ Cu^{II} ion center.[15] A ^{1}H nuclear magnetic resonance (NMR) spectrum of **7** at room temperature exhibits resonances ranging from +65 ppm downfield to –104 ppm upfield. From detailed ^{1}H and/or ^{2}H NMR spectroscopic studies,[18] the upfield (from the diamagnetic region and δ = 0 ppm) resonances are assignable to the Cu^{II}(TMPA) ligand hydrogen resonances, while the pyrrole hydrogens on the iron–porphyrinate shift downfield, and this behavior is ascribed to a S = 2 molecular ground state.

$[(F_8)Fe^{III}–O–Cu^{II}(TMPA)]^+$ (**7**) and other μ-oxo analogues [with ^{6}L, L^{Me_2N}, or L^H ligands; see Chart 1 or Scheme 4 (L^H), below] reversibly protonate to give corresponding μ-hydroxo analogues.[6] For the acid–base conjugate pair $[(F_8)Fe^{III}–(OH)–Cu^{II}(TMPA)]^{2+}$ (**8**) and **7**, the apparent pK_a for the acid form is estimated to be 8 ± 2.5 in a MeCN solvent.[6] For the related complexes, with binucleating ^{6}L ligand, $[(^6L)Fe^{III}–O–Cu^{II}]^+$/$[(^6L)Fe^{III}–(OH)–Cu^{II}]^{2+}$, and with tridentate ligand L^H, $[(F_8)Fe^{III}–(OH)–Cu^{II}(L^H)]^{2+}$/$[(F_8)Fe^{III}–O–Cu^{II}(L^H)]^+$, p$K_a$ values are ~9 and ~9.6, respectively.[6] Thus, the μ-oxo groups in these complexes are very basic, but measurable differences were observed depending upon the ligand architecture or copper–ligand denticity.

The protonation of $[(F_8)Fe^{III}–O–Cu^{II}(TMPA)]^+$ (**7**), $[(^6L)Fe^{III}–O–Cu^{II}]^+$, and $[(F_8)Fe^{III}–O–Cu^{II}(L^H)]^+$ is slow relative to the NMR timescale. Thus, the addition of less than 1 equiv of acid reveals resonances (e.g., porphyrinated pyrrole) because of the individual μ-oxo and μ-hydroxo forms. Protonation causes bending (see Scheme 1) and rehybridization (i.e., sp for oxo and sp^2 for hydroxo) of the M-μ-oxo-M′ core, consistent with relatively slow proton-transfer chemistry.[19,20] The bending/rehydridization is accompanied by bond elongation [see for example Table 1 for Fe^{III}–O(H) and Cu^{II}–O(H) bond lengths in **7** versus **8**]. The extent of antiferromagnetic coupling in the S = 2 systems **7** and **8** is as a consequence also influenced; complex **7** (with $\angle$Fe–O–Cu ~ 180° and shorter/stronger M–O bond distances) possesses a greater electronic interaction (via the μ-oxo ligand) between iron and copper ions than complex **8**.[6] The proton itself makes the oxygen ligand a poor donor because its valence orbitals are greatly lowered in energy, and this would significantly lower *J*.

Generation/Characterization of the Heme/Cu Dioxygen Adduct $[(F_8)Fe^{III}–(O_2^{2-})–Cu^{II}(TMPA)]^+$ (1)

In fact, our real interest was in dioxygen chemistry and O_2 adducts. It seemed likely that such an entity would precede the formation of $[(F_8)Fe^{III}–O–Cu^{II}(TMPA)]^+$ (**7**). In fact, our first success came with the use of the ligand ^{6}L and the low-temperature solution detection and characterization of $[(^6L)Fe^{III}–(O_2^{2-})–Cu^{II}]^+$ (**2**) (Chart 1).[21] Meanwhile, Collman et al.[22] had earlier described the first heme–copper–dioxygen adduct with a superstructured porphyrin possessing a triazacyclononane chelate for copper. Naruta et al.[23] also earlier published results on an adduct similar to **1** (and **6**; Chart 1), possessing a modified TMPA moiety.

Going back, we found that when a 1:1 mixture of $(F_8)Fe^{II}$ and $[(TMPA)Cu^I(RCN)]^+$ were reacted with dioxygen at –40 °C, $[(F_8)Fe^{III}–(O_2^{2-})–Cu^{II}(TMPA)]^+$ (**1**) (Chart 1) is cleanly generated;[24] no homonuclear peroxo products, such as $[\{(TMPA)Cu^{II}\}_2(O_2^{2-})]^{2+}$ or $[(F_8)Fe^{III}–(O_2^{2-})–Fe^{III}(F_8)]$, form. The subsequent peroxo–oxo complex transformation, **1** → $[(F_8)Fe^{III}–O–Cu^{II}(TMPA)]^+$ (**7**) (Scheme 1) involves the evolution of 0.5 equiv of dioxygen, indicative of a peroxide disproportionation reaction,[24] for which we still have little insight. Complex **1** possesses moderate stability at room temperature in a MeCN solvent; it can be isolated as a solid.[25,26] Further characterization includes the fact that (a) its formation occurs in a Fe/Cu/O_2 = 1:1:1 ratio (spectrophotometric titration with O_2), (b) solution mass spectral data give the correct O_2-derived moiety (for which m/z increases by four when formed using $^{18}O_2$), (c) frozen solution resonance Raman (rR) spectroscopy

Scheme 2

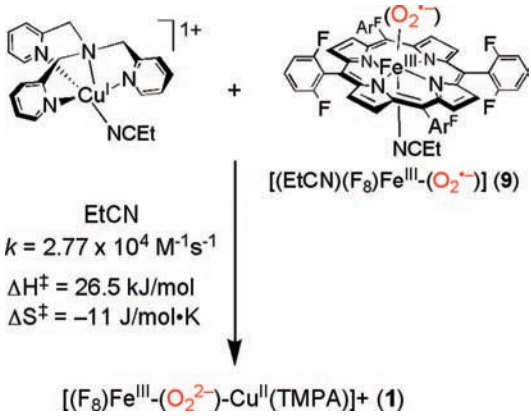

indicates that $\nu_{O-O} = 808$ cm^{-1} and $\Delta^{18}O_2 = -46$ cm^{-1} (413 nm excitation),[27,28] (d) typical high-spin ferric Mössbauer spectroscopic parameters ($\Delta E_Q = 1.14$ mm/s; $\delta = 0.57$ mm/s) are observed, and (e) NMR spectroscopic data (–40 °C, MeCN) giving a pyrrole peak at 68 ppm downfield and pyridyl-H resonances at –11 and –20 ppm upfield are reminiscent of the μ-oxo complex $[(F_8)Fe^{III}–O–Cu^{II}(TMPA)]^+$ (**7**) and characteristic of S = 2 species; in addition, an Evans method magnetic moment determination gave $\mu_B = 5.1$.[24]

In low-temperature oxygenation reactions of $(F_8)Fe^{II}$ with $[(TMPA)Cu^{I}(RCN)]^+$, stopped-flow UV–vis spectroscopy revealed the presence of heme–superoxo $[(S)(F_8)Fe^{III}–(O_2^{\bullet-})]$ (**9**) intermediates, (λ_{max}, 537 nm; S = acetone; $\nu_{O-O} = 1178$, and $\nu_{Fe-O} = 568$ cm^{-1} for S = THF) (Scheme 2), identifiable from separate studies;[29,30] this formed within the mixing time (1 ms) prior to the formation of $[(F_8)Fe^{III}–(O_2^{2-})–Cu^{II}(TMPA)]^+$ (**1**).[24] The known[14,31] copper superoxo species $[(TMPA)Cu^{II}(O_2^{\bullet-})]^+$ may also form, but its detection (λ_{max}, 410 nm) is made very difficult by the presence of the strong heme-based absorptions. A complementary study carried out in EtCN indicates that the heme and copper complexes undergo independent O_2 chemistry (i.e., with known kinetic behavior) and the formation of the heterobinuclear μ-peroxo species **1** occurs as indicated in Scheme 2.[28]

Alternative Synthesis of $[(F_8)Fe^{III}–(O_2^{2-})–Cu^{II}(TMPA)]^+$ (1)

As depicted in Scheme 1, **1** can be also generated in solution or isolated as a solid via a Lewis-acid/Lewis-base reaction. Cobaltocene reduction of the heme–superoxo complex $[(THF)(F_8)Fe^{III}(O_2^{-})]$ affords a η^2-peroxo porphyrinate–Fe^{III} complex $[(F_8)Fe^{III}(O_2^{2-})]^-$ of the type described by Valentine and coworkers.[32] The addition of $[(TMPA)Cu^{II}(MeCN)]^{2+}$ with labile MeCN ligand affords the adduct $[(F_8)Fe^{III}–(O_2^{2-})–Cu^{II}(TMPA)]^+$ (**1**).[25]

Structural/Electronic Descriptions of $[(F_8)Fe^{III}–(O_2^{2-})–Cu^{II}(TMPA)]^+$ (1) and Analogues

The core structure of $[(F_8)Fe^{III}–(O_2^{2-})–Cu^{II}(TMPA)]^+$ (**1**) was investigated using extended X-ray absorption fine structure (EXAFS) spectroscopy on solid as well as in solution samples, in collaboration with Solomon and coworkers.[26] The Cu K-edge first shell was fit with one short (strong) Cu–O/N bond contribution at 1.87 Å, while the second shell was fit to four Cu–N/O contributions at 2.04 Å; these correspond to the Cu^{II}–peroxo and Cu^{II}–TMPA moieties, respectively. The heme environments could be described from Fe K-edge EXAFS with one Fe–O/N contribution (a peroxo O atom) at 1.94 Å and four Fe–N heme–nitrogen contributions at 2.1 Å. From further outer-shell analysis of both Cu and Fe K-edge data, the Fe···Cu distance was determined to be 3.72 Å. From knowledge of Naruta's 2003 breakthrough X-ray structure of the close analogue $[(TMP)Fe^{III}–(O_2^{2-})–Cu^{II}(5Metpa)]^+$ (**6**), having μ-η^2:η^1 peroxo ligation (i.e., side-on bound to Fe^{III} and end-on bound to Cu^{II}; Chart 1),[6,33] the expectation was that **1** was likely to have a similar structure. Our EXAFS analysis indeed was consistent with this structural formulation and was further supported by theoretical calculations (vide infra).

As it turns out, the EXAFS derived Fe···Cu distance in $[(F_8)Fe^{III}–(O_2^{2-})–Cu^{II}(TMPA)]^+$ (**1**) is 0.2 Å shorter than that observed for the close analogue $[(^6L)Fe^{III}–(O_2^{2-})–Cu^{II}]^+$ (**2**)[26] and $[(TMP)Fe^{III}–(O_2^{2-})–Cu^{II}(5Metpa)]^+$ (**6**) (Table 1). Apparently, the presence of an ether linkage to the 6-pyridyl position of the TMPA-like ligand in **2** and an amide linkage to the 5-pyridyl position of the copper ligand in **6** (Chart 1) for both complexes imposes architectural constraints that lead to a preferred Fe···Cu distance of ~4.0 Å. In the case of $[(TMP)Fe^{III}–(O_2^{2-})–Cu^{II}(5Metpa)]^+$ (**6**), the steric (and/or electronic) effects created by the presence of methyl groups at the 5-Me-substituted TPA ligand as well as at the mesityl substituents of the porphyrin ring (Chart 1) may also contribute to the larger Fe···Cu distance {Note, we have shown for μ-oxo complexes $[(L')Fe^{III}–O–Cu^{II}]^+$ with varying ligand constraints (i.e., L′ = ^{6}L or a variation with 5-pyridyl linkage to the TMPA-like moiety) that structural and physical properties can be measurably altered}.[6]

Spin-unrestricted density functional theory (DFT) calculations were performed on the "model" complex $[(P)Fe^{III}–(O_2^{2-})–Cu^{II}(TMPA)]^+$ (P = unsubstituted porphyrinate).[26] The peroxo ligand was found to be coordinated to iron with a side-on ligation, while the copper binds in an end-on fashion, for an overall μ-peroxo-η^2:η^1 coordination mode. In the optimized structure, the calculated Fe···Cu distance was ~0.3 Å longer than that observed experimentally for complex $[(F_8)Fe^{III}–(O_2^{2-})–Cu^{II}(TMPA)]^+$ (**1**) (see Table 1). However, calculations on the same $[(P)Fe^{III}–(O_2^{2-})–Cu^{II}(TMPA)]^+$ compound but with a 3.7 Å Fe···Cu constrained distance resulted in a similar energy (i.e., with only a 3.5 kcal/mol difference), and importantly, the overall μ-η^2:η^1-peroxo coordination mode was retained. The differences found in the optimized calculated structure with respect to the EXAFS experimental results (vida supra) were attributed to the fact that the 2,6-difluorophenyl substituents on the porphyrin ring and the perchlorate counterion were not considered in the calculations.

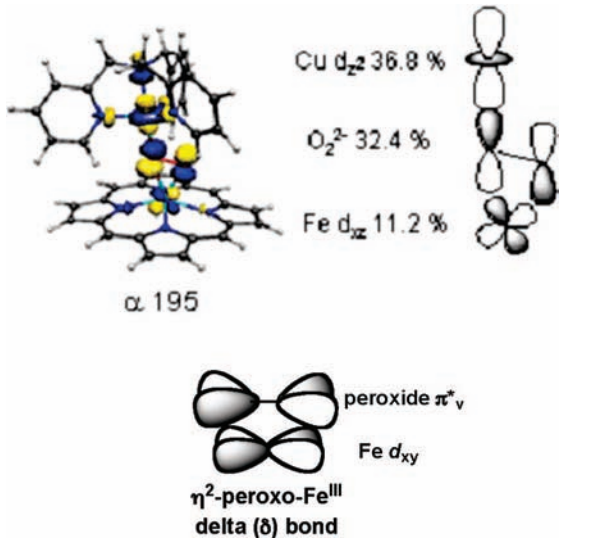

FIGURE 1. (Top) Electronic description for the antiferromagnetic coupling between Fe^{III} and Cu^{II} in $[(P)Fe^{III}–(O_2^{2-})–Cu^{II}(TMPA)]^+$ (P = unsubstituted porphyrinate).[26] We show only the spin-up unoccupied molecular orbital (MO) α-195 (LUMO) of the fully optimized model complex $[(P)Fe^{III}–(O_2^{2-})–Cu^{II}(TMPA)]^+$ and a schematic representation of its major contributions. (Bottom) Depiction of the δ bond of the η^2-peroxo–Fe^{III} moiety.

Solomon's DFT calculations also provided an electronic description of the interactions/bonding within such a $[(P)Fe^{III}–(O_2^{2-})–Cu^{II}(TMPA)]^+$ complex with μ-peroxo-η^2:η^1 moiety.[26] The Cu^{II}–peroxide bond was found to be dominated by electron donation from the π^*_σ orbital of the peroxide into the half occupied Cu d_z^2 orbital (Figure 1). In fact, there are similarities of the Cu^{II}–peroxide bonding to that previously described for $[\{(TMPA)Cu^{II}\}_2(O_2^{2-})]^{2+}$,[36] with peroxide in a *trans*-μ-1,2 geometry. In the case of the side-on bound η^2-peroxo–Fe^{III} moiety, the main interactions are a combination of σ and δ bonds, with the former arising from the donor interaction of the peroxide π^*_σ with the Fe d_{xz} orbital, with the δ bond resulting from the mixing of the peroxide π^*_v with the Fe d_{xy} orbital (Figure 1); the electronic structure here (such as in **1**) is in fact very similar to that also calculated for previously well-known mononuclear $[(P)Fe^{III}–(\eta^2\text{-}O_2^{2-})]^-$ complexes.[37,38] An important finding from the DFT calculations was the description of the origin of the antiferromagnetic coupling between the high-spin Fe^{III} ($S = {}^5/_2$) and Cu^{II} ($S = {}^1/_2$) through the μ-η^2:η^1 peroxide ligand for $[(P)Fe^{III}–(O_2^{2-})–Cu^{II}(TMPA)]^+$. The peroxide π^*_σ interaction with both the half-occupied Cu d_z^2 orbital (η^1) and the high-spin Fe d_{xz} orbital (η^2) provides an effective superexchange pathway (Figure 1).

Structural Changes Due to Tridentate N_3 Ligation for Copper

Because the presence of tri- versus tetradentate chelates profoundly influences the copper–O_2 adduct structure, spectroscopy, and reactivity,[2–5] we sought to probe such effects in heme/Cu/O_2 chemistry. As discussed above, $[(F_8)Fe^{III}–O–Cu^{II}(TMPA)]^+$ (**7**) possesses a near-linear bridging Fe^{III}–O–Cu^{II} unit. However, the geometry is very

Chart 2

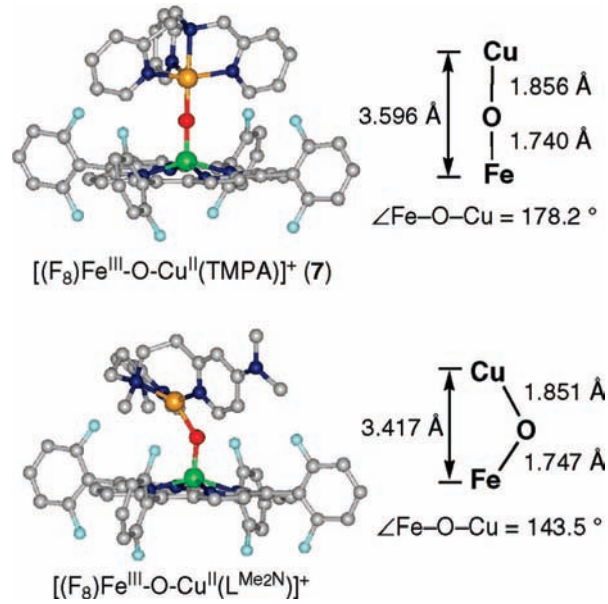

Scheme 3

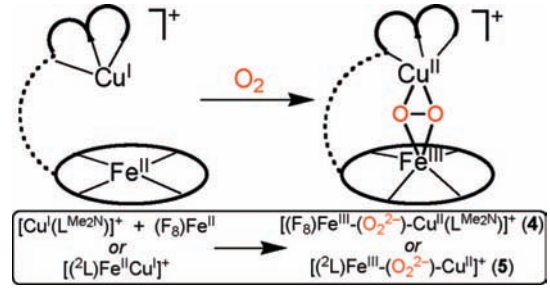

different for the analogue with tridentate L^{Me_2N} chelate, complex $[(F_8)Fe^{III}–O–Cu^{II}(L^{Me_2N})]^+$, which is formed either from an acid–base synthesis or thermal transformation and the loss of ${}^1/_2$ equiv O_2 from μ-peroxo complex $[(F_8)Fe^{III}–(O_2^{2-})–Cu^{II}(L^{Me_2N})]^+$ (**4**)[30] (Chart 1); $[(F_8)Fe^{III}–O–Cu^{II}(L^{Me_2N})]^+$ has a severely bent metal–oxo core (Chart 2).

Pophyrinate–Fe^{III}–(O_2^{2-})–Cu^{II} Complexes with Tridentate Cu Chelates

As indicated in Chart 1, heme–peroxo–copper complexes also form with three N ligands bound to copper. These are generated in the same manner as discussed for **1** or **2**, by the oxygenation of reduced component mononuclear heme and copper complexes [producing $[(F_8)Fe^{III}–(O_2^{2-})–Cu^{II}(L^{Me_2N})]^+$ (**4**)][30] or binuclear Fe^{II}–Cu^I assemblies [giving $[(^2L)Fe^{III}–(O_2^{2-})–Cu^{II}]^+$ (**5**)][35,39] (Chart 1 and Scheme 3). These peroxo complexes are also S = 2 spin systems, with high-spin Fe^{III} coupled to Cu^{II}. In Figure 2, NMR and rR spectroscopic data are highlighted for $[(^2L)Fe^{III}–(O_2^{2-})–Cu^{II}]^+$ (**5**). The latter confirms the peroxo formulation, with $\nu_{O–O}$ = 752 and 747 cm^{-1}, for **4** and **5**, respectively (Chart 1). The striking finding is that these values are considerably reduced from those observed for **1** and **2** with tetradentate Cu chelates, with

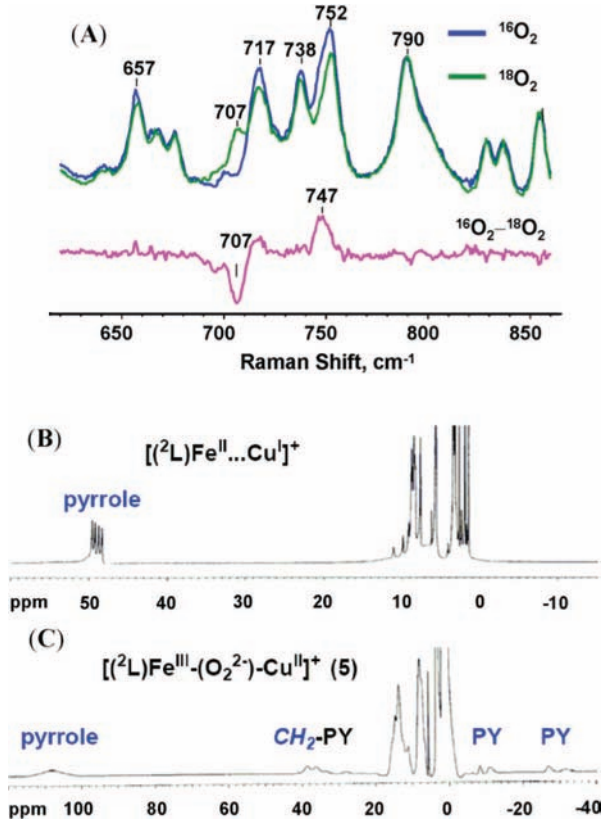

FIGURE 2. (A) Resonance Raman spectra of [(^{2}L)Fe^{III}–(O_2^{2-})–Cu^{II}]$^+$ (**5**), formed by the oxygenation of [(^{2}L)Fe^{II} ··· Cu^{I}]$^+$ with $^{16}O_2$ and $^{18}O_2$, respectively. The lower part represents the difference spectrum showing $\nu_{O-O} = 747$ cm^{-1} and $\Delta(^{18}O_2) = -40$ cm^{-1}. ^{1}H NMR spectra (acetone-d_6) of (B) [(^{2}L)Fe^{II} ··· Cu^{I}]$^+$ ($\delta_{pyrrole} \sim 50$ ppm; room temperature) and (C) [(^{2}L)Fe^{III}–(O_2^{2-})–Cu^{II}]$^+$ (**5**) ($\delta_{pyrrole} \sim 110$ ppm; –90 °C).

values lowered by 50–60 cm^{-1} (Chart 1). This indicates a weakened O–O peroxo bond, because of a different heme–peroxo–copper core structure (vide infra).

Side-On/Side-On Peroxo Ligation with Tridentate Ligands for Copper

Chemical reasoning/logic and preliminary EXAFS data reveal that [(F_8)Fe^{III}–(O_2^{2-})–Cu^{II}(L^{Me_2N})]$^+$ (**4**) and [(^{2}L)Fe^{III}–(O_2^{2-})–Cu^{II}]$^+$ (**5**) possess a μ-η^2:η^2-peroxo ligation (Chart 1 and Scheme 3). In peroxo–dicopper(II) complexes, tetradentate Cu ligands lead to end-on μ-1,2-peroxo ligation, but with tridentate chelates, side-on μ-η^2:η^2-peroxo coordination is common (Chart 3).[3,4] The former possesses relatively normal ν_{O-O} values, typically above 800 cm^{-1} (Chart 3). However, the latter side-on complexes have reduced (<760 cm^{-1}) ν_{O-O} values (Chart 3), ascribed to back bonding from copper to the peroxo antibonding π^* orbital, which considerably weakens the O–O bond.[40] Thus, the μ-η^2:η^1-peroxo ligation (end-on to Cu^{II}) now established for complexes **1** and **6** (vide supra) possessing tetradentate chelates is in accordance with the expectations. Further, high-spin heme–Fe^{III} peroxo complexes [(P)Fe^{III}(O_2^{2-})]$^-$ exhibit ν_{O-O} stretching frequencies very close to 800 cm^{-1}

Chart 3

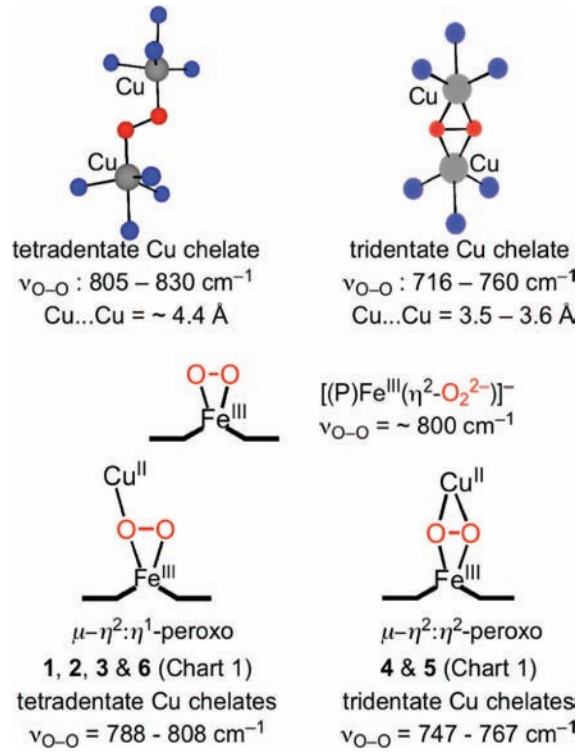

Chart 4

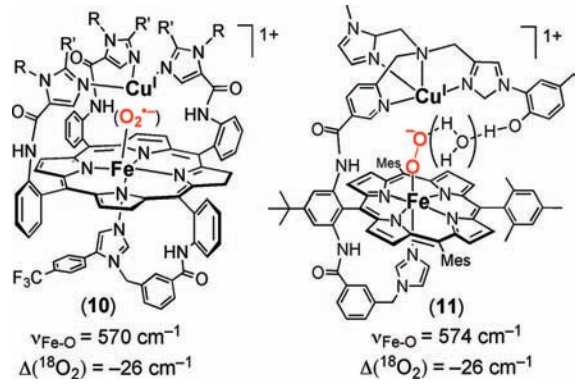

(Chart 3).[37] Thus, to achieve a lowering of the O–O stretching frequency from the 800 cm^{-1} region [for **1** and **6** or [(P)Fe^{III}(O_2^{2-})]$^-$] to near 750 cm^{-1} as seen in **4** and **5**, these latter complexes likely possess side-on/side-on μ-η^2:η^2-peroxo heme–copper coordination (Chart 3). EXAFS spectroscopic analysis carried out on [(^{2}L)Fe^{III}–(O_2^{2-})–Cu^{II}]$^+$ (**5**) gives a Fe ··· Cu distance of 3.6 Å, consistent with this conclusion; this distance is typically observed for μ-η^2:η^2 dicopper(II) complexes.[4]

Dynamics and Intermediates in Heme–Peroxo–Copper Complex Formation

Collman et al.[41] and more recently Naruta et al.[9] have generated heme–superoxide (Fe^{III}–$O_2^{\bullet-}$) moieties, which are stable in the presence of a neighboring Cu^{I} complex (Chart 4); they do not readily "close" with further electron transfer to give μ-peroxo products. Compound **10** (Chart 4) was generated by the oxygenation of the fully reduced heterobinuclear Fe^{II}/Cu^{I} complex and is relatively stable

Scheme 4

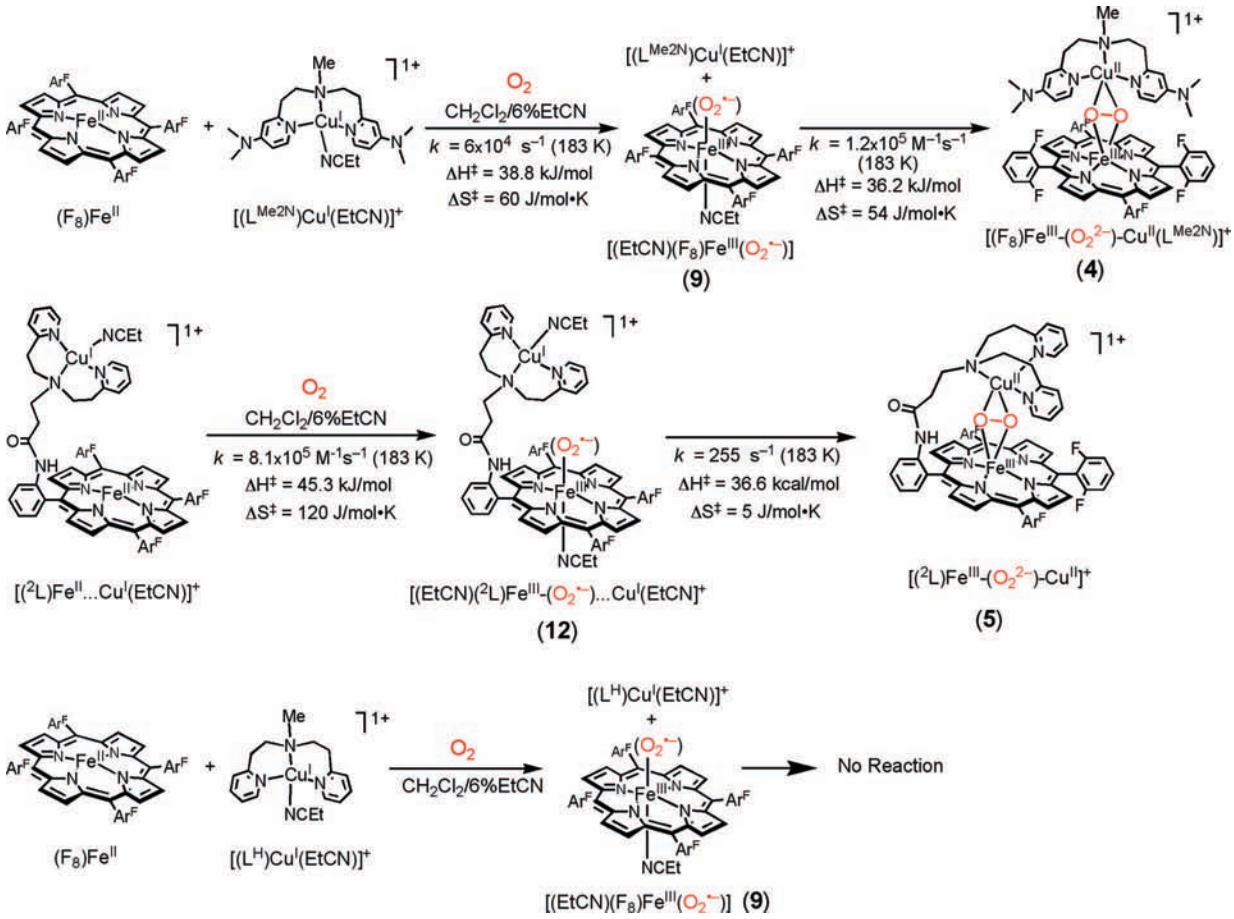

at room temperature; this then may model the initial O_2 intermediate observed in C*c*O (referred to as "Oxy" or intermediate **A**).[41] Complex **11** formed after conversion of a μ-peroxo Fe^{III}–(O_2^{2-})–Cu^{II} intermediate initially observable at –70 °C.[9]

In low-temperature stopped-flow kinetic/spectroscopic studies, we also observe short-lived Fe^{III}–$O_2^{\bullet-}$ ··· Cu^{I} species or mixtures forming *prior to* the generation of μ-peroxo Fe^{III}–(O_2^{2-})–Cu^{II} products **1**,[24,28] **2**,[21] **4**,[30] and **5** (Chart 1).[39] A particularly nice comparison of complexes and data (Scheme 4) comes from studies employing a variety of tridentate ligands for copper.

The reaction of $(F_8)Fe^{II}$ and $[(L^{Me_2N})Cu^{I}]^+$ with O_2 leads first (–90 °C) to the heme–superoxo complex $[(EtCN)(F_8)Fe^{III}(O_2^{\bullet-})]$ (**9**).[29] This subsequently decays to form $[(F_8)Fe^{III}$–(O_2^{2-})–$Cu^{II}(L^{Me_2N})]^+$ (**4**) (Scheme 4).[30] For the case of $[(^2L)Fe^{II}Cu^{I}]^+$, the Fe^{II}/O_2 reaction is measurably faster (because of an increase in $\Delta S^{\ddagger}$); a transient Fe^{III}–superoxo/Cu^{I} species $[(EtCN)(^2L)Fe^{III}$–($O_2^{\bullet-}$) ··· Cu^{I}-(EtCN)]$^+$ (**12**) then decays via the reaction with the Cu^{I}–ligand moiety to give $[(^2L)Fe^{III}$–(O_2^{2-})–$Cu^{II}]^+$ (**5**) (Scheme 4). The kinetics of the formation of [(solvent)-(P)$Fe^{III}(O_2^{\bullet-})$] (e.g., **9**) are independent of the presence of any copper complex.[39] The activation enthalpies for the formation of **4** and **5** are essentially the same (~36 kJ/mol); both involve electron-transfer reduction and binding by Cu^{I} (Scheme 4). This is despite the formation of **4** being an intermolecular reaction but in particular involving a strongly reducing ligand–copper(I) complex $[(L^{Me_2N})$-$Cu(EtCN)]^+$ (with dimethylamino 4-pyridyl substituents), while the other reaction to form **5** involves the intramolecular reaction of the much less electron-donating (to copper) bis[2-(2-pyridylethyl]amine moiety (Scheme 4).[39,42]

A heme–peroxo–copper complex analogue to **4** or **5** does not form when a mixture of $(F_8)Fe^{II}$ and $[(L^{H})Cu^{I}$-$(EtCN)]^+$ is oxygenated (Scheme 4).[39] Nitrile solvent binding inhibits the O_2 reaction and makes such a complex with the L^H chelate a poor reductant; in contrast, L^{Me_2N} renders $[(L^{Me_2N})Cu^{I}(EtCN)]^+$ a sufficiently good reductant to lead to μ-peroxo product $[(F_8)Fe^{III}$–(O_2^{2-})–$Cu^{II}(L^{Me_2N})]^+$ (**4**). However, if the L^H chelate is tethered to the porphryin periphery (as in ^{2}L), the intramolecular nature of the subsequent reaction of the $[(L^{H})Cu^{I}(EtCN)]^+$ fragment with the heme–superoxo moiety leads to successful redox chemistry, giving $[(^2L)Fe^{III}$–(O_2^{2-})–$Cu^{II}]^+$ (**5**).

Heme–Peroxo–Copper Complexes with the Imidazole–Phenol Cross-Link

Because the His–Tyr moiety bound to copper in the C*c*O active site appears to play a key role in the reductive O–O cleavage process,[6] we designed and introduced imidazole–phenol moieties within either tri- or tetradentate chelates for copper.[43] For example, low-temperature

Scheme 5

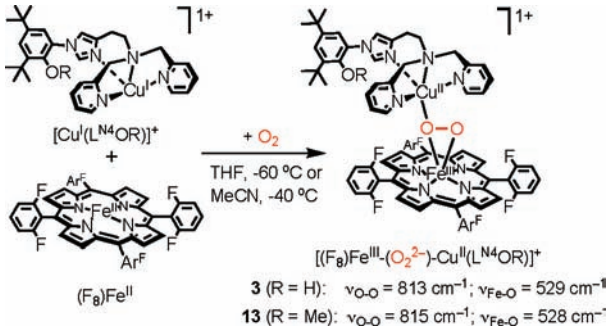

Scheme 6

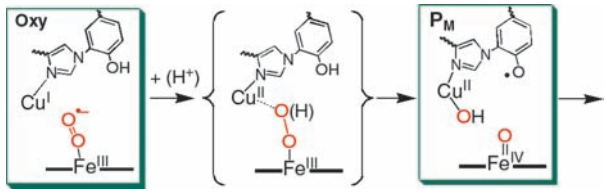

oxygenation of $[Cu^{I}(L^{N4}OR)]^{+}$ with $(F_8)Fe^{II}$ leads to the formation of heme–peroxo–copper species $[(F_8)Fe^{III}$–(O_2^{2-})–$Cu^{II}(L^{N4}OR)]^{+}$ **3** or **13** (Scheme 5),[44] which possess similar ν_{O-O} values, also close to that seen for $[(F_8)Fe^{III}$–(O_2^{2-})–$Cu^{II}(TMPA)]^{+}$ (**1**) ($\nu_{O-O} = 808\ cm^{-1}$; Chart 1), without any imidazole–phenol group. Thus, the phenol moiety in $[(F_8)Fe$–(O_2^{2-})–$Cu^{II}(L^{N4}OH)]^{+}$ (**3**) does not interact with the μ-peroxo group. Also, we have not observed O–O cleavage products (i.e., phenoxy radical or Fe^{IV}=O), with those possibly facilitated by the phenol donation of a hydrogen atom within **3**.

Other research groups have also generated interesting imidazole–phenol or similar copper chelates for study,[6,9,45,46] as relevant to C*c*O active-site chemistry.[6] For Naruta's complex **11** (Chart 4), O–O cleavage also is not triggered.[9]

Reductive Cleavage of the O–O Bond

Thus, heme–copper/O_2 reactivity studies should also aim to probe reductive O–O cleavage chemistry. In C*c*O, this takes place between the detectable **A** ("Oxy", Fe^{III}–superoxo complex) and $\mathbf{P_M}$ (Fe^{IV}=O, i.e., ferryl) enzyme states (Scheme 6). Four electrons are required to break an O–O bond, eventually producing two water molecules (eq 1). However, only three electrons are readily available from the reduced bimetallic site (two from iron, $Fe^{II} \rightarrow Fe^{IV}$, and one from copper, $Cu^{I} \rightarrow Cu^{II}$). The tyrosine cross-linked to the Cu_B histidine–imidazole ligand (see Chart 1) or a nearby tryptophan may provide the fourth electron.[6,47] Calculations[12] suggest that an "unstable" μ-peroxo or (protonated) hydroperoxo heme–copper structure that forms (having an associated water network from the tyrosine; Chart 1 or Scheme 6) is reduced by the tyrosine, leading to O–O bond cleavage.

Thus, can synthetic Fe^{III}–(O_2^{2-})–Cu^{II} or Fe^{III}–$(O_2^{\bullet-})$ $\cdots$ Cu^{I} assemblies, such as those described in this Account, be subjected to conditions that lead to reductive O–O bond cleavage, to probe this reaction that is key to C*c*O function and important in general for metal-ion-mediated O_2 activation (vide supra)? As described above, synthetically appended imidazole–phenol "cofactors" adjacent to copper centers have not yet yielded O–O reductive cleavage chemistry. However, Collman et al.[46] recently reported that their Fe^{III}–$(O_2^{\bullet-})$ $\cdots$ Cu^{I} complex **10** (Chart 4) reacts with exogenously added hindered phenols, leading to phenoxyl radicals and the formation of a Fe^{IV}=O (ferryl) species, as observed in the enzyme. We have also recently described very similar chemistry advances,[48] as well as the fact that the addition of a reductant [a copper(I) complex], proton source, and bulky imidazole (as an axial heme ligand) to $[(F_8)Fe^{III}(O_2^{2-})]^{-}$ (Scheme 1) triggers O–O bond cleavage, resulting in ferryl and cupric hydroxide formation. Systematic investigations aimed at obtaining detailed insights into these kinds of O–O cleavage chemistries are in progress.

Summary/Conclusions

In this Account, we have tried to overview our work and that of others in the generation and characterization of heme/copper/O_2 adducts, studied to provide basic insights into dioxygen reactivity at heme–Cu centers. Information obtained may be relevant to C*c*O enzyme active-site chemistry. A number of Fe^{III}–(O_2^{2-})–Cu^{II} or Fe^{III}–$(O_2^{\bullet-})$ $\cdots$ Cu^{I} assemblies have been generated; dynamics of their formation have been studied; and physical and electronic structures and bonding have been elucidated in some cases. Considerable future efforts are needed to firm up structural formulations discussed, fully elucidate electronic structure, and compare and contrast reactivity patterns for heme/copper/O_2 adducts as influenced by copper–ligand denticity, binucleating ligand architectural variations, or the presence of a heme axial "base" (i.e., an imidazole or a pyridine donor). While we now have some notions of the heme–Cu–O_2 structure in high-spin environments, what structures form as low-spin systems and how do high-spin versus low-spin systems react? Such considerations are likely relevant to the O–O reductive cleavage process, and indications are that such heme–Cu-mediated chemistry is amenable to detailed investigation.

Note Added in Proof New chemistry relevant to the above discussion on O–O bond cleavage was recently published by Collman and coworkers {*Science* **2007**, *315*, 1565–1568; *J. Am. Chem. Soc.* **2007**, *129*, 5794–5795}. These reports describe synthetically derived heme–copper assemblies possessing a copper–ion ligated imidazole–phenol moiety. The authors ascertain from their chemical and spectroscopic data that O_2-reactions of their fully reduced complexes lead to reductive O–O cleavage, affording a ferryl–copper(II)-phenoxyl radical species, as proposed for cyt. c oxidase turnover chemistry.

References

(1) Walker, F. A.; Simonis, U. In *Encyclopedia of Inorganic Chemistry*, 2nd ed.; King, R. B., Ed.; John Wiley and Sons Ltd.: New York, 2005; Vol. 4, pp 2390–2521.

(2) Itoh, S. Mononuclear copper active-oxygen complexes. *Curr. Opin. Chem. Biol.* **2006**, *10*, 115–122.

(3) Quant Hatcher, L.; Karlin, K. D. Oxidant types in copper–dioxygen chemistry: The ligand coordination defines the Cu_n–O_2 structure and subsequent reactivity. *J. Biol. Inorg. Chem.* **2004**, *9*, 669–683.

(4) Mirica, L. M.; Ottenwaelder, X.; Stack, T. D. P. Structure and spectroscopy of copper–dioxygen complexes. *Chem. Rev.* **2004**, *104*, 1013–1045.

(5) Lewis, E. A.; Tolman, W. B. Reactivity of dioxygen–copper systems. *Chem. Rev.* **2004**, *104*, 1047–1076.

(6) Kim, E.; Chufán, E. E.; Kamaraj, K.; Karlin, K. D. Synthetic models for heme–copper oxidases. *Chem. Rev.* **2004**, *104*, 1077–1133.

(7) Collman, J. P.; Boulatov, R.; Sunderland, C. J.; Fu, L. Functional analogues of cytochrome *c* oxidase, myoglobin, and hemoglobin. *Chem. Rev.* **2004**, *104*, 561–588.

(8) Chishiro, T.; Shimazaki, Y.; Tani, F.; Naruta, Y. Selective formation of a stable μ-peroxo ferric heme–Cu^{II} complex from the corresponding μ-oxo Fe^{III}–Cu^{II} species with hydrogen peroxide. *Chem. Commun.* **2005**, 1079–1081.

(9) Liu, J. G.; Naruta, Y.; Tani, F. A functional model of the cytochrome *c* oxidase active site: Unique conversion of a heme–μ-peroxo–Cu^{II} intermediate into heme–superoxo/Cu^{I}. *Angew. Chem., Int. Ed.* **2005**, *44*, 1836–1840.

(10) Lee, Y.; Karlin, K. D. In *Concepts and Models in Bioinorganic Chemistry*; Metzler-Nolte, N., Kraatz, H.-B., Eds.; Wiley-VCH: New York, 2006; pp 363–395.

(11) Decker, A.; Solomon, E. I. Dioxygen activation by copper, heme and non-heme iron enzymes: Comparison of electronic structures and reactivities. *Curr. Opin. Chem. Biol.* **2005**, *9*, 152–163.

(12) Blomberg, M. R. A.; Siegbahn, P. E. M. Different types of biological proton transfer reactions studied by quantum chemical methods. *Biochim. Biophys. Acta* **2006**, *1757*, 969–980.

(13) Kitajima, N. Synthetic approach to the structure and function of copper proteins. *Adv. Inorg. Chem.* **1992**, *39*, 1–77.

(14) Karlin, K. D.; Kaderli, S.; Zuberbühler, A. D. Kinetics and thermodynamics of copper(I)/dioxygen interaction. *Acc. Chem. Res.* **1997**, *30*, 139–147.

(15) Karlin, K. D.; Nanthakumar, A.; Fox, S.; Murthy, N. N.; Ravi, N.; Huynh, B. H.; Orosz, R. D.; Day, E. P. X-ray structure and physical properties of the oxo-bridged complex $[(F_8\text{-TPP})Fe\text{–}O\text{–}Cu(TMPA)]^+$, F_8-TPP = tetrakis(2,6-difluorophenyl)porphyrinate^{2-}, TMPA = tris(2-pyridylmethyl)amine: Modeling the cyhtochrome *c* oxidase Fe–Cu heterodinuclear active site. *J. Am. Chem. Soc.* **1994**, *116*, 4753–4763.

(16) Counteranions typically employed to afford organic solvent solubility are PF_6^-, ClO_4^-, and $B(C_6F_5)_4^-$.

(17) Lee, S. C.; Holm, R. H. Synthesis and characterization of an asymmetric bridged assembly containing the unsupported [Fe^{III}–O–Cu^{II}] bridge: An analogue of the binuclear site in oxidized cytochrome *c* oxidase. *J. Am. Chem. Soc.* **1993**, *115*, 11789–11798.

(18) Nanthakumar, A.; Fox, S.; Murthy, N. N.; Karlin, K. D. Inferences from the ^{1}H-NMR spectroscopic study of an antiferromagnetically coupled heterobinuclear Fe(III)–X–Cu(II) $S = 2$ spin system (X = O^{2-}, OH^-). *J. Am. Chem. Soc.* **1997**, *119*, 3898–3906.

(19) Fox, S.; Nanthakumar, A.; Wikström, M.; Karlin, K. D.; Blackburn, N. J. XAS structural comparisons and reversibly interconvertible oxo and hydroxo bridged heme–copper oxidase model compounds. *J. Am. Chem. Soc.* **1996**, *118*, 24–34.

(20) Kramarz, K. W.; Norton, J. R. Slow proton-transfer reactions in organometallic and bioinorganic chemistry. *Prog. Inorg. Chem.* **1994**, *42*, 1–65.

(21) Ghiladi, R. A.; Ju, T. D.; Lee, D.-H.; Moënne-Loccoz, P.; Kaderli, S.; Neuhold, Y.-M.; Zuberbühler, A. D.; Woods, A. S.; Cotter, R. J.; Karlin, K. D. Formation and characterization of a high-spin heme–copper dioxygen (peroxo) complex. *J. Am. Chem. Soc.* **1999**, *121*, 9885–9886.

(22) Collman, J. P.; Herrmann, P. C.; Boitrel, B.; Zhang, X.; Eberspacher, T. A.; Fu, L.; Wang, J.; Rousseau, D. L.; Williams, E. R. A synthetic analogue for the oxygen binding site in cytochrome *c* oxidase. *J. Am. Chem. Soc.* **1994**, *116*, 9783–9784.

(23) Sasaki, T.; Nakamura, N.; Naruta, Y. Formation and spectroscopic characterization of the peroxoFe^{III}–Cu^{II} complex. A modeling reaction of the heme–Cu site in cytochrome *c* oxidase. *Chem. Lett.* **1998**, 351–352.

(24) Ghiladi, R. A.; Hatwell, K. R.; Karlin, K. D.; Huang, H.-w.; Moënne-Loccoz, P.; Krebs, C.; Huynh, B. H.; Marzilli, L. A.; Cotter, R. J.; Kaderli, S.; Zuberbühler, A. D. Dioxygen reactivity of mononuclear heme and copper components yielding a high-spin heme–peroxo–Cu complex. *J. Am. Chem. Soc.* **2001**, *123*, 6183–6184.

(25) Chufán, E. E.; Karlin, K. D. An iron–peroxo porphyrin complex. New synthesis and nucleophilic reactivity toward a Cu(II) complex giving a heme–peroxo–copper adduct. *J. Am. Chem. Soc.* **2003**, *125*, 16160–16161.

(26) del Rio, D.; Sarangi, R.; Chufán, E. E.; Karlin, K. D.; Hedman, B.; Hodgson, K. O.; Solomon, E. I. Geometric and electronic structure of the heme–peroxo–copper complex $[(F_8TPP)Fe^{III}\text{–}(O_2^{2-})\text{–}Cu^{II}(TMPA)](ClO_4)$. *J. Am. Chem. Soc.* **2005**, *127*, 11969–11978.

(27) Complex $[(F_8)Fe^{III}\text{–}(O_2^{2-})\text{–}Cu^{II}(TMPA)]^+$ (**1**) was also investigated using 676 nm excitation; the $\nu_{O\text{–}O}$ (now observed at 810 cm^{-1}) and two different M–O vibrations at 533 and 511 cm^{-1} were clearly identified. Normal coordinate analysis and DFT calculations further support that the 810 cm^{-1} mode is a dominant (80 %) O–O stretching vibration, whereas the 533 and 511 cm^{-1} modes correspond essentially to the $\nu_{Fe\text{–}O}$ (where O is the oxygen only bound to Fe; see the structure description of **1**, below) and to an asymmetric ν_{as}(Fe–O–Cu) vibration, respectively. See ref 28.

(28) Ghiladi, R. A.; Chufán, E. E.; del Rio, D.; Solomon, E. I.; Krebs, C.; Huynh, B. H.; Huang, H.-w.; Moënne-Loccoz, P.; Kaderli, S.; Honecker, M.; Zuberbühler, A. D.; Marzilli, L.; Cotter, R. J.; Karlin, K. D. Further insights into the spectroscopic, electronic structure, and kinetics of formation of the heme–peroxo–copper complex $[(F_8TPP)\text{-}Fe^{III}\text{–}(O_2^{2-})\text{–}Cu^{II}(TMPA)]^+$. *Inorg. Chem.* **2007**, *46*, 3889–3902.

(29) Ghiladi, R. A.; Kretzer, R. M.; Guzei, I.; Rheingold, A. L.; Neuhold, Y.-M.; Hatwell, K. R.; Zuberbühler, A. D.; Karlin, K. D. Reversible dioxygen binding to $(F_8TPP)Fe^{II}/O_2$ reactivity studies {F_8TPP = tetrakis(2,6-difluorophenyl)porphyrinate}: Spectroscopic (UV–visible and NMR) and kinetic study of solvent-dependent (Fe/O_2 = 1:1 or 2:1) reversible O_2-reduction and ferryl formation. *Inorg. Chem.* **2001**, *40*, 5754–5767.

(30) Kim, E.; Helton, M. E.; Wasser, I. M.; Karlin, K. D.; Lu, S.; Huang, H.-w.; Moënne-Loccoz, P.; Incarvito, C. D.; Rheingold, A. L.; Honecker, M.; Kaderli, S.; Zuberbühler, A. D. Superoxo, μ-peroxo and μ-oxo complexes from heme/O_2 and heme–copper/O_2 reactivity studies: Copper–ligand influences in cytochrome *c* oxidase models. *Proc. Natl. Acad. Sci. U.S.A.* **2003**, *100*, 3623–3628.

(31) Maiti, D.; Fry, H. C.; Woertink, J. S.; Vance, M. A.; Solomon, E. I.; Karlin, K. D. A 1:1 copper–dioxygen adduct is an end-on bound superoxo copper(II) complex which undergoes oxygenation reactions with phenols. *J. Am. Chem. Soc.* **2007**, *129*, 264–265.

(32) Wertz, D. L.; Valentine, J. S. Nucleophilicity of iron–peroxo porphyrin complexes. *Struct. Bonding* **2000**, *97*, 37–60.

(33) Chishiro, T.; Shimazaki, Y.; Tani, F.; Tachi, Y.; Naruta, Y.; Karasawa, S.; Hayami, S.; Maeda, Y. Isolation and crystal structure of a peroxo-bridged heme–copper complex. *Angew. Chem., Int. Ed.* **2003**, *42*, 2788–2791.

(34) Ghiladi, R. A.; Huang, H. W.; Moënne-Loccoz, P.; Stasser, J.; Blackburn, N. J.; Woods, A. S.; Cotter, R. J.; Incarvito, C. D.; Rheingold, A. L.; Karlin, K. D. Heme–copper/dioxygen adduct formation relevant to cytochrome *c* oxidase: Spectroscopic characterization of $[(^6L)Fe^{III}(O_2^{2-})\text{–}Cu^{II}]^+$. *J. Biol. Inorg. Chem.* **2005**, *10*, 63–77.

(35) Kim, E.; Shearer, J.; Lu, S.; Moënne-Loccoz, P.; Helton, M. E.; Kaderli, S.; Zuberbühler, A. D.; Karlin, K. D. Heme/Cu/O_2 reactivity: Change in $Fe^{III}\text{–}(O_2^{2-})\text{–}Cu^{II}$ unit peroxo binding geometry effected by tridentate copper chelation. *J. Am. Chem. Soc.* **2004**, *126*, 12716–12717.

(36) Baldwin, M. J.; Ross, P. K.; Pate, J. E.; Tyeklár, Z.; Karlin, K. D.; Solomon, E. I. Spectroscopic and theoretical studies of an end-on peroxide-bridged coupled binuclear copper(II) model complex of relevance to the active sites in hemocyanin and tyrosinase. *J. Am. Chem. Soc.* **1991**, *113*, 8671–8679.

(37) Selke, M.; Sisemore, M. F.; Valentine, J. S. The diverse reactivity of peroxy ferric porphyrin complexes of electron-rich and electron-poor porphyrins. *J. Am. Chem. Soc.* **1996**, *118*, 2008–2012.

(38) However, the calculations show a switch in d-orbital ordering for $[(P)Fe^{III}\text{–}(\eta^2\text{-}O_2^{2-})]^-$ compared to the copper-containing complex $[(P)Fe^{III}\text{–}(O_2^{2-})\text{–}Cu^{II}(TMPA)]^+$ (**1**), with the latter possessing the expected orbital energy ordering for high-spin iron(III).

(39) Kim, E.; Helton, M. E.; Lu, S.; Moënne-Loccoz, P.; Incarvito, C. D.; Rheingold, A. L.; Kaderli, S.; Zuberbühler, A. D.; Karlin, K. D. Tridentate copper ligand influences on heme–peroxo–copper formation and properties: Reduced, superoxo, and μ-peroxo iron/copper complexes. *Inorg, Chem.* **2005**, *44*, 7014–7029.

(40) Solomon, E. I.; Tuczek, F.; Root, D. E.; Brown, C. A. Spectroscopy of binuclear dioxygen complexes. *Chem. Rev.* **1994**, *94*, 827–856.

(41) Collman, J. P.; Sunderland, C. J.; Berg, K. E.; Vance, M. A.; Solomon, E. I. Spectroscopic evidence for a heme–superoxide/Cu(I) intermediate in a functional model of cytochrome *c* oxidase. *J. Am. Chem. Soc.* **2003**, *125*, 6648–6649.
(42) Zhang, C. X.; Liang, H.-C.; Kim, E.-i.; Shearer, J.; Helton, M. E.; Kim, E.; Kaderli, S.; Incarvito, C. D.; Zuberbühler, A. D.; Rheingold, A. L.; Karlin, K. D. Tuning copper–dioxygen reactivity and exogenous substrate oxidations via alterations in ligand electronics. *J. Am. Chem. Soc.* **2003**, *125*, 634–635.
(43) Kamaraj, K.; Kim, E.; Galliker, B.; Zakharov, L. N.; Rheingold, A. L.; Zuberbuehler, A. D.; Karlin, K. D. Copper(I) and copper(II) complexes possessing cross-linked imidazole–phenol ligands: Structures and dioxygen reactivity. *J. Am. Chem. Soc.* **2003**, *125*, 6028–6029.
(44) Kim, E.; Kamaraj, K.; Galliker, B.; Rubie, N. D.; Moënne-Loccoz, P.; Kaderli, S.; Zuberbühler, A. D.; Karlin, K. D. Dioxygen reactivity of copper and heme–copper complexes possessing an imidazole–phenol cross-link. *Inorg. Chem.* **2005**, *44*, 1238–1247.
(45) Nagano, Y.; Liu, J. G.; Naruta, Y.; Ikoma, T.; Tero-Kubota, S.; Kitagawa, T. Characterization of the phenoxyl radical in model complexes for the Cu_B site of cytochrome *c* oxidase: Steady-state and transient absorption measurements, UV resonance Raman spectroscopy, EPR spectroscopy, and DFT calculations for M-BIAIP. *J. Am. Chem. Soc.* **2006**, *128*, 14560–14570.
(46) Collman, J. P.; Decréau, R. A.; Sunderland, C. J. Single-turnover intermolecular reaction between a Fe^{III}–superoxide–Cu^{I} cytochrome *c* oxidase model and exogeneous Tyr244 mimics. *Chem. Commun.* **2006**, 3894–3896.
(47) MacMillan, F.; Budiman, K.; Angerer, H.; Michel, H. The role of tryptophan 272 in the *Paracoccus denitrificans* cytochrome *c* oxidase. *FEBS Lett.* **2006**, *580*, 1345–1349.
(48) Puiu, S. C.; Chufan, E. E.; Mondal, B.; Karlin, K. D. Heme/Cu complexes as functional models for the active site of cytochrome *c* oxidase. Abstracts of Papers, 230th ACS National Meeting, Washington, D.C., Aug 28–Sept 1, 2005, 230, U2157–U2158, INOR-307.

AR700031T